

The Diels-Alder Cycloaddition Reaction of some Substituted Furans and *E*-1,2-Bis(phenylsulfonyl)ethylene

Odón Arjona,^{a,*} Fátima Iradier,^a Rosario M. Mañas,^a Joaquín Plumet,^{a,*}
^aUniversidad Complutense, Facultad de Química, Departamento de Química Orgánica I,
E-28040 Madrid, Spain.

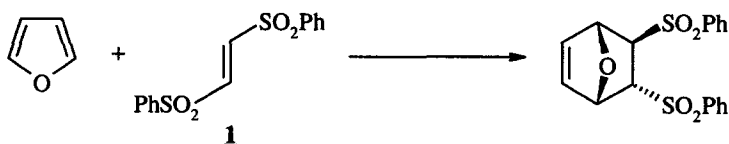
Xavier Grabuleda,^b and Carlos Jaime^{b,*}
^bUniversitat Autònoma de Barcelona, Departament de Química,
E-08193 Bellaterra, Spain.

Received 31 December 1997; revised 18 May 1998; accepted 3 June 1998

Abstract: The Diels-Alder cycloaddition between several 2-, and 3-substituted furans and *E*-1,2-bis(phenylsulfonyl)ethylene have been carried out in high yields. Stereoselectivity observed in the case of 2-substituted furans has been explained by means of the MM3-transition state model. The model had to be refined for 2-methoxyfuran due to the asymmetry induced over the transition state geometry by the electron-donating methoxyl group. Selectivity in 2-substituted furans arose by interactions between the 2-substituent and the sulfonyl groups (steric repulsion with the *cis*-sulfonyl or long-range favourable interactions with the *trans*-sulfonyl). © 1998 Elsevier Science Ltd. All rights reserved.

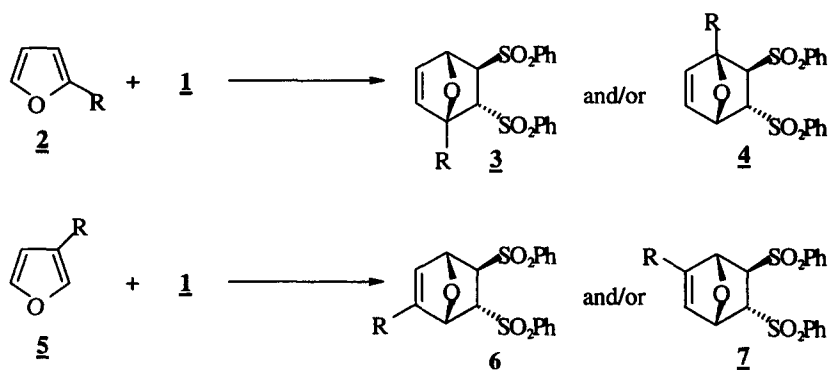
INTRODUCTION

The Diels-Alder cycloaddition reaction of furan and substituted furan derivatives with different dienophiles constitutes a powerful tool for the synthesis of complex molecules¹. In the case of the reaction of *E*-1,2-bis(phenylsulfonyl)ethylene, **1**, and furan (Scheme 1), first described by De Lucchi et al.², the resulting adducts have been used as intermediates for the synthesis of compounds such as the aminocyclitol fragment of Pancratistatin³, and (+)-Pinitol⁴.



Scheme 1.

In order to gain information about the extension of this reaction to different substituted furan derivatives for further application to the preparation of other synthetic targets, we have considered the cycloaddition reactions of **1** and several 2-, and 3-substituted furan derivatives (Scheme 2). The experimental results of these reactions together with their interpretation in terms of the MM2-transition state model for the process constitute the objective of this report.



RESULTS AND DISCUSSION

The reaction of compound **2** with the dienophile **1** was totally stereoselective (Table 1) affording cycloadducts **3**. Structural determination of cycloadducts **3** and **4** was based on the splitting patterns observed in ^1H NMR (300 MHz) for the bridgehead proton in both compounds. In the ^1H NMR spectra for compounds **3a**, **3b** and **3c**, H-4 shows a multiplicity of doublet ($J= 1.8$ or 1.5 Hz). This value confirms that the coupling is with the vinylic proton H-3. In addition, H-5 appears as a doublet in all compounds ($J= 4.4$ or 4.8 Hz) by exclusive coupling with H-6. Both coupling constants indicate that the coupling between H-4 and H-5 does not exist confirming the proposed structure (Fig 1a). For compounds **3d** and **3e**, we observed a singlet at 5.28 or 5.26 ppm respectively, corresponding to H-4. Besides, H-5 appears as a doublet in all cases ($J= 4.4$ Hz) by coupling exclusively with H-6. Both facts confirm the proposed structures for cycloadducts **3** (Fig 1b).

It should be pointed out that for compounds **4**, H-4 would appear as a doublet by coupling with H-5 or as a double doublet by coupling with H-5 and H-3 (Fig 1c).

Table 1. Diels-Alder Reactions of 2- and 3-Substituted Furans, **2a-e**.

Entry	2	Ratio 3:4 ^{a)}	Overall yield ^{b)}
1	2a , R=Me	100:0	100
2	2b , R=OMe	100:0	100
3	2c , R=CH ₂ OH	70:30 ^{c)}	100
4	2d , R=CH ₂ OBn	100:0	78
5	2e , R=CH ₂ SH	100:0	100

a) Determined by 300 MHz ^1H -NMR spectroscopy. b) Isolated yields. c) Larger reaction time provides with a 100:0 ratio.

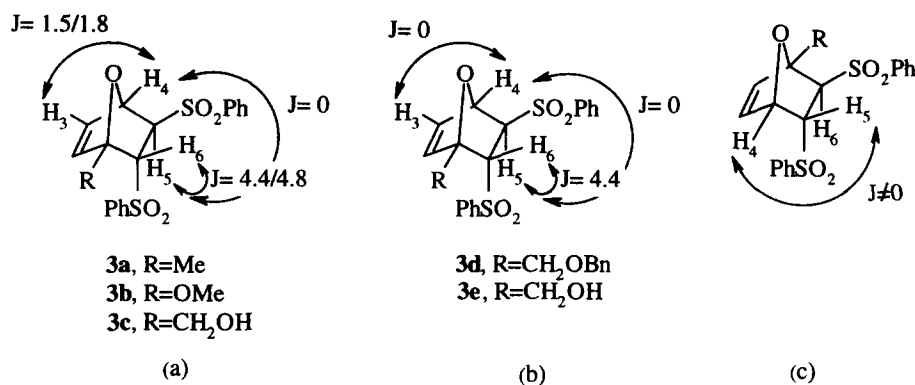
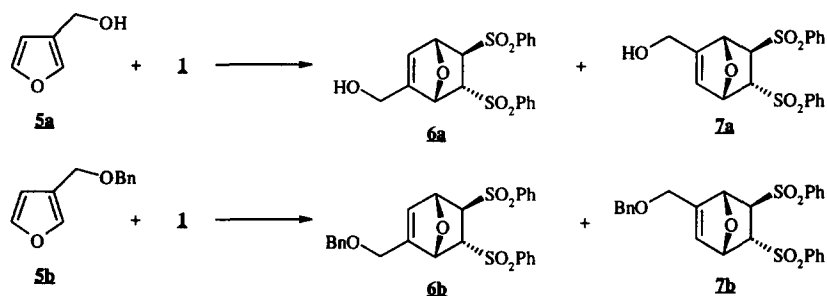


Fig 1. Coupling constants between specific protons; a) stereoisomers **3a-c**; b) stereoisomers **3d-e**; c) stereoisomers **4**.

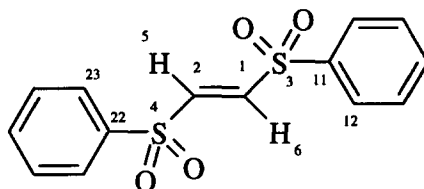
In the case of the 3-substituted furan derivatives, a dramatic loss of selectivity was observed. Thus, the reaction of furan derivatives **5a**, and **5b** with **1** affords a nearly equimolar amount of the two cycloadducts **6** and **7** in 76% and 87% isolated yields, respectively (Scheme 3). In both cases, separation of the isomers by column chromatography was not possible, and then configurational assignment of compounds **6** and **7** remains undetermined.



Scheme 3.

Conformational analysis of *E*-1,2-bis(phenylsulfonyl)ethylene, **1**:

Full conformational analysis of **1** was carried out with the MM3* force field⁵. All rotatable bonds (four in total) were driven in successive steps from +180° to -180° at 15° increments. Each structure was minimized in all variables except the one being driven. All obtained energy minima were fully optimized using the Polac-Ribiere conjugate gradient⁶ minimization algorithm with enough cycles to ensure convergence. The aim of this conformational analysis was the location of stable conformers to subsequently adjust in the basic transition state used in the molecular mechanics calculations. Table 2 shows the relative energy and torsion angle values for all obtained conformers. Only conformer **1-c3** presents a parallel disposition of the phenylsulfonyl groups leading to a favourable π -stacking interaction between the phenyl fragments.

Table 2. Relative Energy (kcal mol⁻¹) and Torsion Angles (Degrees) for the Computed Conformers of **1**.

Conformer	S.E. ^{a)}	w1 ^{b)}	w2 ^{b)}	w3 ^{b)}	w4 ^{b)}
1-c1	0.0	99.7	99.2	99.3	100.3
1-c2	0.2	99.3	-101.4	76.9	99.0
1-c3	0.0	-108.1	-108.1	69.9	70.0
1-c4	0.2	-101.6	99.2	98.4	76.0

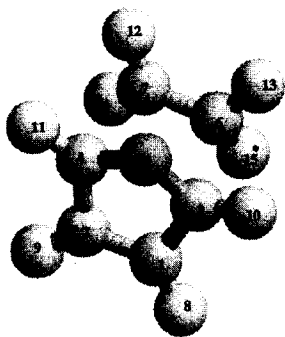
a) S.E. = relative steric energy. b) w1 = 5-2-4-22, w2 = 3-1-6-11, w3 = 1-6-11-12, w4 = 2-4-22-23.

Ab initio transition structure and MM3 models:*

The well-known MM2-transition state method of Houk et al.⁷ has been used throughout this work under the frame of MacroModel v. 5.0 package⁸. Following Houk's approach, a transition state for the reaction between furan and ethylene (the simplest reactants) computed by high level *ab initio* calculations (B3LYP/6-31G*) was used⁹. MM3* has been the selected force field to reproduce the *ab initio* transition structure, and two new atom types (one for each pair of reacting atoms) have been parameterised for. The reacting ethylene carbon atom had a slightly greater sp² character in the transition state than the reacting carbon atom of furan; their van der Waals parameters were taken from C2 (sp²) and C3 (sp³) atom type of MM3* force field, respectively. The same correlation was made for the stretching parameters using the interatomic distances from *ab initio* calculations as equilibrium distances. Standard bond lengths for forming bonds were taken as 2.150 Å. Bending parameters for reacting carbon atoms, and for furan sp² carbon atoms were set using the angle values of the *ab initio* calculations to ensure the degree of pyramidalization of these atoms observed in the *ab initio* structure. Finally, those torsion parameters involving bonds between reacting carbon atoms were set equal to zero¹⁰. Table 3 contains the main geometrical features obtained from the *ab initio* calculations as well as those obtained by MM3* with our new parameterization.

Transition Structures for Diels-Alder Reactions:

All possible transition states for the reaction of **1** with **2a-e** were constructed over the basic transition state model. All combinations between computed conformers of **1** (four in total) and each structure for **2a-e** were made. Consistently, the MM3* force field was enlarged to include the necessary parameters to carry out molecular mechanics optimizations. Other parameters were adapted from the MM3* force field as explained above. Table 4 contains the MM3* parameters used to model the simplest reactants (furan and ethylene).

Table 3. Main Geometrical Features Obtained for the TS between Furan and Ethylene by *ab initio* and by MM3* Calculations.


Bond Lengths					
	<i>ab initio</i>	MM3*		<i>ab initio</i>	MM3*
1-2	1.379	1.360	3-10	1.083	1.084
1-3	1.419	1.428	6-7	1.400	1.392
1-8	1.082	1.102	6-13	1.085	1.087
3-5	1.373	1.363	6-15	1.087	1.087
3-6	2.150	2.150			

Bond Angles					
	<i>ab initio</i>	MM3*		<i>ab initio</i>	MM3*
1-2-4	105.8	105.8	5-3-10	114.9	114.8
1-2-9	127.9	128.0	6-7-12	120.1	120.1
1-3-5	108.2	108.3	6-7-14	119.1	119.1
1-3-10	127.9	128.0	13-6-15	114.5	114.5
3-1-8	125.6	125.6			
3-5-4	103.3	103.3			

Torsion Angles					
	<i>ab initio</i>	MM3*		<i>ab initio</i>	MM3*
1-2-4-5	17.9	17.8	5-3-1-8	170.7	170.0
1-2-4-11	162.8	162.8	8-1-2-9	0.0	0.0
1-3-5-4	28.5	28.3	8-1-3-10	25.8	25.0
3-1-2-4	0.0	0.0	12-7-6-13	0.0	0.0
3-1-2-9	-171.0	171.9	12-7-6-15	150.5	150.7
3-5-4-1	-178.5	-178.5	14-7-6-15	0.0	0.0

Standard deviation (σ): Bond Lengths = ± 0.01 Å, Bond Angles = $\pm 0.03^\circ$ and Torsion Angles = $\pm 0.45^\circ$.

Table 4. Parameters for new atom types in MM3* force field as implemented in MacroModel (ethylene C are T1, and reacting furan C are T2).

	Bond Length ^a	Force const. ^b	Bond moment ^c		Bond Length	Force const.	Bond moment
C2-T2	1.419	7.7	0.	T2-H1	1.083	5.15	-0.9
T1-H1	1.086	5.15	-0.6	T2-O3	1.373	10.	1.07
T1-T1	1.4	7.5	0.	T2-T1	2.15	999.99	0.

	Angle ^d	Bend const. ^e		Angle	Bend const.		Angle	Bend const.	Bend-bend ^e
C2-T2-H1	128.	999.99	H1-T1-T2	94.	100.	T1-T1-T2	100.1	100.	
C2-T2-O3	108.3	100.	H1-T2-T1	107.	100.	T2-C2-H1	125.6	100.	
C2-T2-T1	99.6	100.	O3-T2-H1	114.9	100.	T2-O3-T2	103.3	100.	
C2=C2-T2	105.8	999.99	O3-T2-T1	91.2	100.	O3-T2-O3	108.6	0.54	0.24
H1-T1-H1	114.5	100.	T1-T1-H1	120.1	100.				

	V1 ^f	V2 ^f	V3 ^f		V1	V2	V3		V1	V2	V3
C2-T2-O3-T2	0.	40.	0.	H1-T2-T1-H1	0.	0.	0.	T2-C2=C2-H1	0.	10.	0.
C2-T2-T1-H1	0.	0.	0.	O3-T2-C2-H1	0.	15.	0.	T2-C2=C2-T2	-0.3	8.	0.
C2-T2-T1-T1	0.	0.	0.	O3-T2-T1-H1	0.	0.	0.	T2-O3-T2-H1	-0.1	2.7	0.8
C2=C2-T2-H1	0.25	9.	-0.55	O3-T2-T1-T1	0.	0.	0.	T2-O3-T2-T1	0.	0.	0.
C2=C2-T2-O3	0.	15.	0.6	T1-T1-T2-H1	0.	0.	0.	T2-T1-T1-H1	0.	0.	0.
C2=C2-T2-T1	0.	0.	0.	T1-T2-C2-H1	0.	0.	0.	T2-T1-T1-T2	0.	0.	0.
H1-C2-T2-H1	0.	11.5	0.								

a) Bond length in Å. b) Force constant in mdyn/Å. c) Bond moment in debye. d) Bond angle in degree. e) Bend force constant in mdyn/rad**2. f) V1, V2 and V3 in kcal/mol

General assumptions are that substituents will not substantially alter the geometry of transition structures and that selectivity is caused by steric interactions existing between substituents of both furan and dienophile in diastereomeric transition structures. Full conformational analysis for furan substituents were carried out over all constructed transition structures. Obtained energy minima (1, 13, 6, and 10 for **2b-e**, respectively) were optimised separately in vacuum and with GB/SA solvation model¹¹ using CHCl₃ as solvent.

Computational results for transition structures are gathered in Table 6. Computed energies (in kcal mol⁻¹) are relative to the most stable transition structure of each reaction. Populations were computed by using Boltzmann distribution at 25° without considering entropy contributions.

Reaction between **1** and **2a**:

No conformational analysis was undertaken over the transition structure of this reaction due to the nature of the substituent. Computations (in vacuum and GB/SA) gave the **1-c3/2a** transition structure as the most stable. The computed population afforded **3a/4a** ratios of 97.2/2.8 (in vacuum) and 98.3/1.7 (with solvation model) in excellent agreement with experimental results. The contribution of bending and van der Waals energy terms produced the energy difference between products **3a** and **4a**. The electrostatic term also contributed to the energy difference but in a lesser degree. Table 5 contains the relative energy differences between these energetic terms for in vacuum and GB/SA calculations. Absolute values of increments decreased when the GB/SA solvation model is used. Fig. 2 shows the stereoview of the most stable computed conformers for **3a** and **4a** in vacuum calculations.

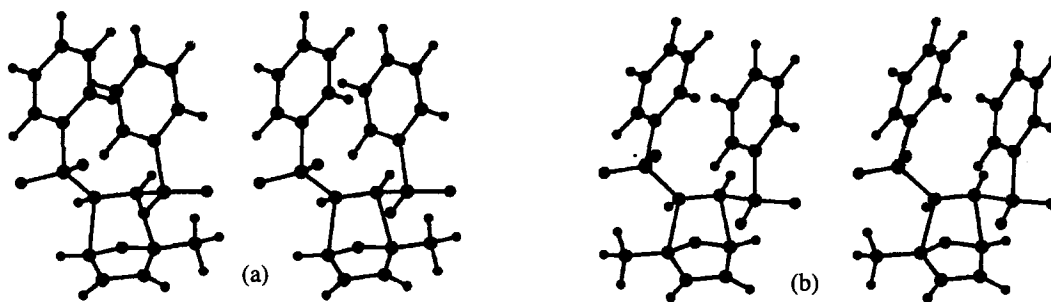


Fig. 2. Stereoview of the most stable computed (in vacuum) transition structures for the **1/2a** reaction. (a) structure producing **3a**; (b) structure producing **4a**.

The preferred transition structure corresponded to the less hindered one, with the methyl group not interacting with the sulfonyl substituent of **1**. The orientation of the phenyl rings in **1** allowed a stabilising π stacking interaction¹² with distances between phenyl rings of 3.7 Å, and 3.6 Å for **3a**, and **4a**, respectively.

Reaction between **1** and **2b**:

The conformational analysis of the rotatable bond (C-OCH₃) of **2b** was carried out over each of the built transition structures (four in total) by driving the torsion angle w_1 (Fig. 3) from 0° to 360° at 15° increments. Computed population of each structure produced by full energy minimisation of the resulting conformers (Table

6) gave a **3b/4b** ratio of 51.2/48.8 or 51.1/48.9 for the in vacuum or the GB/SA method, respectively, not in good agreement with experimental results (100/0, see Table 1). This deviation will be discussed in detail.

Table 5. Relative Energy Differences (kcal mol⁻¹) between Products **3a** and **4a** for the Bending, Electrostatic and van der Waals Steric Energy Terms in Vacuum and GB/SA Solvation Model Calculations.

	$\Delta E(4a-3a)$	
	In vacuum	GB/SA
Bending	4.33	1.09
Electrostatic	0.92	0.33
Van der Waals	3.45	0.77

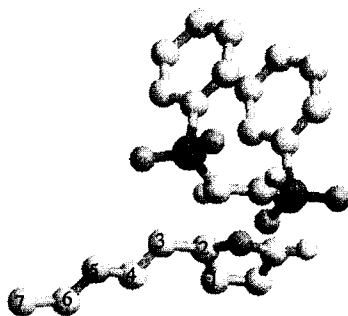


Fig. 3. General structure showing the selected atoms for conformational analysis:
w1=1-2-3-4, w2=2-3-4-5, w3=3-4-5-6, w4=4-5-6-7.

Reaction between **1** and **2c**:

Starting material **2c** (R= -CH₂OH) contained two rotatable bonds. A full torsional energy surface covering has been carried out over all **1/2c** transition structures. Torsion angles w1 and w2 (Fig. 3) were gradually changed from 0° to 360° at 15° steps over each of the constructed transition structures producing **3c** and **4c**. Final results (Table 6) indicated a total of 13 conformers for **3c** distributed on 4, 4, 3, and 2 for the **1-c1**, **1-c2**, **1-c3**, and **1-c4** conformers, respectively. Results for **4c** indicated a smaller number of conformers (8 in total) distributed in 2 for each conformer of **1**. In spite of getting the same name (c1, c2, ...) no relation exists between the obtained conformers. For in vacuum calculations, three conformers giving to **3c** were within 1.2 kcal mol⁻¹ while the second most stable conformer for **4c** is 3.04 kcal mol⁻¹ away from the global energy minimum. This, and the smaller number of conformers obtained, indicated **4c** was more congested than **3c**. For the GB/SA calculations, results are quite different: the energy gap between conformers in **3c** increased as well as in **4c** (see Table 6). It was noteworthy that in all cases the transition structures for **3c** and **4c** came from the **1-c3** conformer that presented π -stacking interactions between the phenylsulfonyl rings. The computed population gave rise to a **3c/4c** ratio of 78/22 and 94.9/6.1 for in vacuum or with GB/SA, respectively. The energy terms responsible for the energy differences between **3c** and **4c** were the bending, electrostatic and van der Waals

terms for both in vacuum and GB/SA calculations. However, while bending and van der Waals terms favoured **3c**, the electrostatic term favoured **4c** but always with a lower absolute value. While in vacuum calculations were in good agreement with experimental results, the effect of CHCl_3 (as described in the GB/SA model) modified the distribution. Table 6 showed that for **3c**, conformers **2c-c9** and **2c-c10** presented different population distribution for in vacuum (43.2%-28.8%), and with solvent calculations (7.7%-75.7%). One hydrogen bond between the hydroxymethyl hydrogen and the sulfonyl oxygen was present in **2c-c9**, but not in **2c-c10**. This hydrogen bond represents (in vacuum) an extra stabilisation of $2.67 \text{ kcal mol}^{-1}$ for **2c-c9** over **2c-c10**; value which decreased to $0.16 \text{ kcal mol}^{-1}$ with the GB/SA solvation model. All other energetic terms (bending and torsion) produced a greater difference between **2c-c9** and **2c-c10** in GB/SA solvation model and favoured the **2c-c10** conformer ($\Delta E_{\text{bending}} \text{ c10} - \text{c9} = -0.92 \text{ kcal mol}^{-1}$ and $\Delta E_{\text{torsion}} \text{ c10} - \text{c9} = -0.73 \text{ kcal mol}^{-1}$). Fig. 4 shows, explicitly, the stacked disposition for the aromatic rings of the dienophile in transition structures producing **3c** and **4c** with GB/SA solvation model calculations.

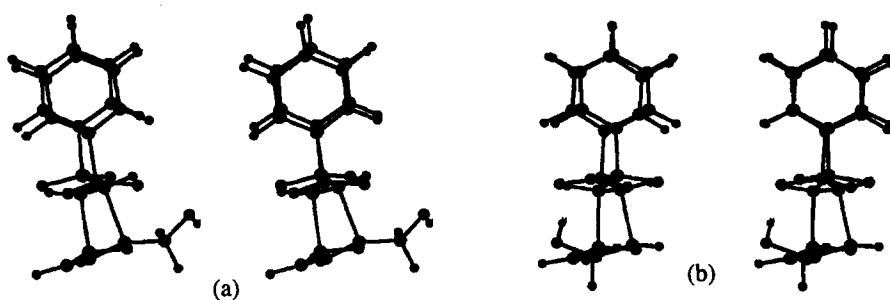


Fig. 4. Stereoview of the global energy minima for the $1/2c$ computed transition structures showing the π stacking orientation of aromatic rings as computed using the GB/SA solvation model: (a) structure producing **3c** (b) structure producing **4c**.

Reaction between **1** and **2d**:

Compound **2d** presents a larger number of rotatable bonds (four in total). The methodology for covering the conformational space has been slightly modified in this case: four consecutive dihedral drivers (one for each rotatable torsion angle of the $-\text{CH}_2\text{-OBn}$ group (w_1 , w_2 , w_3 and w_4 , Fig. 2) were carried out starting from the previous rotamer at increments of 15° . This grid-search gave a total of 6 conformers for transition structures producing **3d** and only 4 for those giving rise to **4d**. Again, transition structures for **4d** seem to be slightly more congested than those for **3d**. Use of solvent model did not change the relative stability order (see Table 6), and the transition structures corresponding to **3d** were always more stable than those for **4d**. The **1-c3** conformer led again to the most stable transition structures.

The transition structure **1-c3/2d-c4** (which produces **3d**) presents π -stacking interactions between phenylsulfonyl rings (3.7 \AA between aromatic rings). The substituent folding brings the benzyl group near to the stacked phenyl rings (Fig. 5). This benzyl group interacts in a 'type T' edge to face manner¹³ with the phenylsulfonyl rings (distances between phenylsulfonyl and benzyl rings protons were around 3.2 \AA). None of the transition structures producing **4d** presented this folding. However, the chain substituent modified their torsion angles to put the CH_2OBn group distant from the sulfonyl unit.

Table 6. Computed Relative Energy (kcal mol⁻¹) and Population Analysis (in parenthesis, %) for the Different Transition Structures (TS) of Reactions between **1** and **2a-e**.

Reactant	TS	<u>In vacuum</u>		<u>GB/SA</u>		
		3a	4a	3a	4a	
2a	1-c1/2a	7.12 (0.0)	11.72 (0.0)	6.24 (0.0)	7.41 (0.0)	
	1-c2/2a	3.66 (0.2)	4.98 (0.0)	2.95 (0.7)	2.39 (0.0)	
	1-c3/2a	0.00 (96.5)	2.10 (2.8)	0.00 (96.1)	4.42 (1.7)	
	1-c4/2a	3.16 (0.5)	7.67 (0.0)	2.47 (1.5)	11.18 (0.0)	
2b		3b	4b	3b	4b	
	1-c1/2b	3.17 (0.2)	7.66 (0.0)	2.63 (0.6)	7.20 (0.0)	
	1-c2/2b	1.82 (2.2)	3.08 (0.3)	1.04 (8.2)	2.34 (0.99)	
	1-c3/2b	0.00 (48.5)	0.00 (48.5)	0.08 (41.7)	0.00 (47.8)	
	1-c4/2b	3.16 (0.2)	3.70 (0.1)	2.63 (0.6)	3.15 (0.2)	
2c-c1		3c	4c	3c	4c	
	1-c1/2c-c1	7.49 (0.0)	9.78 (0.0)	8.17 (0.0)	10.18 (0.0)	
	-c2	1-c1/2c-c2	7.14 (0.0)	12.82 (0.0)	6.26 (0.0)	12.58 (0.0)
	-c3	1-c1/2c-c3	7.42 (0.0)		7.04 (0.0)	
	-c4	1-c1/2c-c4	8.43 (0.0)		7.85 (0.0)	
	-c5	1-c2/2c-c5	3.35 (0.1)	3.42 (0.1)	2.44 (1.2)	3.61 (0.2)
	-c6	1-c2/2c-c6	3.64 (0.1)	5.92 (0.0)	2.48 (1.1)	5.55 (0.0)
	-c7	1-c2/2c-c7	5.43 (0.0)		5.16 (0.0)	
	-c8	1-c2/2c-c8	4.94 (0.0)		4.63 (0.0)	
	-c9	1-c3/2c-c9	0.00 (43.2)	0.41 (21.6)	1.35 (7.7)	1.52 (5.8)
	-c10	1-c3/2c-c10	0.24 (28.8)	3.04 (0.2)	0.00 (75.7)	3.50 (0.2)
	-c11	1-c3/2c-c11	1.23 (5.4)		1.45 (6.5)	
	-c12	1-c4/2c-c12	3.29 (0.2)	5.88 (0.0)	3.95 (0.1)	6.56 (0.0)
-c13	1-c4/2c-c13	3.15 (0.2)	8.80 (0.0)	2.41 (1.3)	8.84 (0.0)	
2d-c1		3d	4d	3d	4d	
	1-c1/2d-c1	10.12 (0.0)	14.30 (0.0)	8.15 (0.0)	12.53 (0.0)	
	-c2	1-c2/2d-c2	2.67 (1.1)	7.66 (0.0)	2.45 (1.5)	5.68 (0.0)
	-c3	1-c3/2d-c3	3.19 (0.4)	4.80 (0.0)	1.94 (3.6)	3.68 (0.2)
	-c4	1-c3/2d-c4	0.00 (98.4)		0.00 (94.6)	
	-c5	1-c4/2d-c5	4.30 (0.1)	10.25 (0.0)	3.97 (0.1)	8.77 (0.0)
-c6	1-c4/2d-c6	6.22 (0.0)		4.41 (0.0)		
2e-c1		3e	4e	3e	4e	
	1-c1/2e-c1	7.19 (0.0)	13.20 (0.0)	6.44 (0.0)	12.81 (0.0)	
	-c2	1-c1/2e-c2	8.41 (0.0)	13.53 (0.0)	7.70 (0.0)	13.13 (0.0)
	-c3	1-c2/2e-c3	3.50 (0.2)	6.39 (0.0)	3.01 (0.6)	5.88 (0.0)
	-c4	1-c2/2e-c4	5.83 (0.0)	6.79 (0.0)	5.38 (0.0)	6.28 (0.0)
	-c5	1-c2/2e-c5	5.78 (0.0)	7.12 (0.0)	5.32 (0.0)	6.63 (0.0)
	-c6	1-c2/2e-c6	4.76 (0.0)	6.41 (0.0)	4.12 (0.1)	5.92 (0.0)
	-c7	1-c2/2e-c7	5.13 (0.0)	3.52 (0.2)	4.68 (0.0)	3.86 (0.1)
		1-c3/2e-c7				
	-c8	1-c3/2e-c8	0.00 (90.5)	3.96 (0.1)	0.00 (90.5)	4.30 (0.1)
-c9	1-c3/2e-c9	1.41 (8.4)	9.17 (0.0)	1.50 (7.4)	9.03 (0.0)	
	1-c4/2e-c9					
-c10	1-c4/2e-c10	3.17 (0.4)	9.48 (0.0)	2.60 (1.1)	9.36 (0.0)	

Computed **3d/4d** ratio were now of 100/0 and 99.8/0.2 for in vacuum or GB/SA calculations, respectively, in perfect agreement with experimental results. As for **3c** and **4c**, bending and van der Waals energy terms stabilised transition structures giving rise to **3d** while the electrostatic term tended to stabilise those for **4d**. Different behaviour was observed with the GB/SA solvation model. The electrostatic term inverts its previous tendency and causes a relative stabilisation of **3d** by 4.39 kcal mol⁻¹ while for in vacuum calculations this term destabilised **3d** by -1.23 kcal mol⁻¹ relative to **4d**. The introduction of the solvent favours the folding of the substituent chain in compound **3d**.

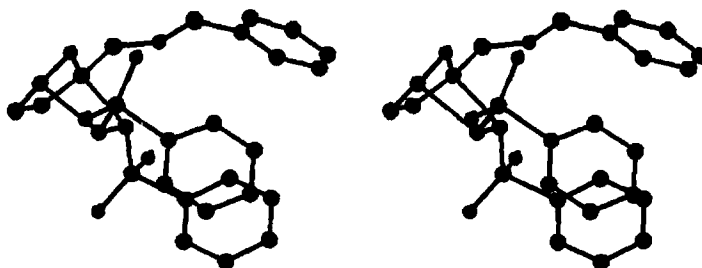


Fig. 5. Stereoview of the energy minimum transition structures producing **3d**. Hydrogen atoms have been removed for clarity.

Reaction between 1 and 2e:

Conformational analysis for the transition structures constructed were carried out as for **2c**. The rotatable bonds were w1 and w2 (Fig. 2). A total of 10 conformers were obtained for transition structures producing **3e** distributed on 2, 5, 2, and 1 for the **1-c1**, **1-c2**, **1-c3**, and **1-c4** conformers, respectively. Results for **4e** also indicated a total of 10 conformers distributed on 2, 4, 3, and 2 for the **1-c1**, **1-c2**, **1-c3**, and **1-c4** conformers, respectively. The **3e** transition structures were always (in vacuum and with solvation model) the most stable. Again, the phenylsulfonyl groups produced a π -stacking interactions and one hydrogen bond between the furan ring oxygen and the thiol group hydrogen was observed in **3e** minimum transition structure for the **1-c3** conformer (see Fig. 6). Computed **3e/4e** ratio were of 99.6/0.3 and 99.7/0.2 for in vacuum or GB/SA calculations, respectively, in perfect agreement with experimental results. Electrostatic and hydrogen bonding terms stabilised **3e** over **4e** (in vacuum) by 1.55, and 3.25 kcal mol⁻¹, respectively. However, product **4e** was stabilised due to the van der Waals term by 1.52 kcal mol⁻¹ with respect to **3e**. This stabilisation was interpreted by the congested conformation observed in product **3e**: the formation of the hydrogen bond between the furan oxygen and the thiol hydrogen led to short interaction distances (1.8 Å) between these groups. For GB/SA calculations, the electrostatic term remained unaltered but the hydrogen bonding term decreased the absolute relative energy difference between **3e/4e** but it still favoured the **3e** product. It is noteworthy that the van der Waals term for the solvent calculations favoured the **3e** product. The study of the transition structure showed that the distance between the furan oxygen and the thiol hydrogen increased to be 2.4 Å.

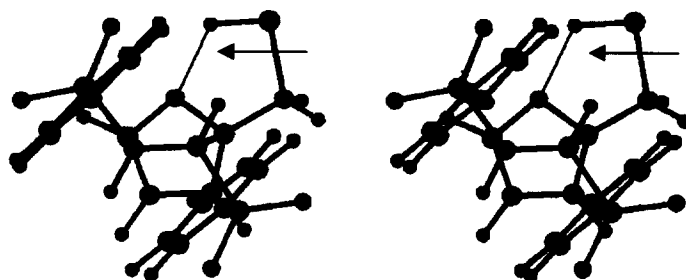


Fig. 6. Stereoview of the most stable transition structure (in vacuum calculations) for **3e**. Arrows mark the hydrogen bond between the furan oxygen and the thiol hydrogen.

DISCUSSION

The MM3* force field parameterisation developed for dealing with carbon atoms present in transition states for Diels-Alder reactions has obtained good agreement with experimental results for **2a**, **2c**, **2d**, and **2e** dienes. The exception arrived for diene **2b**, for which computations afforded an equimolar amount of cycloadducts **3b** and **4b** while experimental results determined an exclusive formation of **3b**. The presence of an oxygen atom directly connected to one reacting carbon atom of the furan ring may distort the symmetry of the transition state used previously. In order to improve the results, new *ab initio* calculations (with the same methodology)¹⁴ were undertaken to locate the transition state for the reaction between 2-hydroxyfuran and ethylene. Table 7 shows the main geometrical features obtained for the TS between 2-hydroxyfuran and ethylene in our *ab initio* calculation. The newly computed transition state presents two different distances between reacting carbon atoms (C4---C7 was shorter than C3---C6). The MM3* force field was again modified to adjust it to these geometrical changes, and this new parameterisation led to an exact modelling of the transition state (Table 7). The introduction of a new atom type¹⁵ was needed to reproduce the two different forming bond distances; four bending angles were to be redefined for the transition state structure involving the O3-T2-O3(H2), C2-T2-O3(H2), T1-T2-O3(H2) and T2-O3-H2 angles; finally, torsion parameters were adapted from previous force field parameters. The transition state structure for the reaction between **1** and **2b** was thus computed again introducing the OCH₃ group and following the methodology explained above. Once the simplest transition state was successfully modelled, the methodology used for reaction between **1** and **2c-e** was used. Computational results are gathered in Table 8. All of the transition structures presented the CH₃ group of OCH₃ substituent distant from the sulfonyl group. Results indicated that the conformer **1-c3** again gave the most stable transition structure showing a favourable π stacking interaction between the phenylsulfonyl rings.

The population distribution of **3b/4b** presented a ratio of 86.2/13.8 for the in vacuum (or 84.7/15.3 for the GB/SA method), values closer to the experimental results (100/0). Fig. 7 shows a stereoview representation for the minima transition structures giving rise to **3b** and to **4b** as obtained in vacuum calculations.

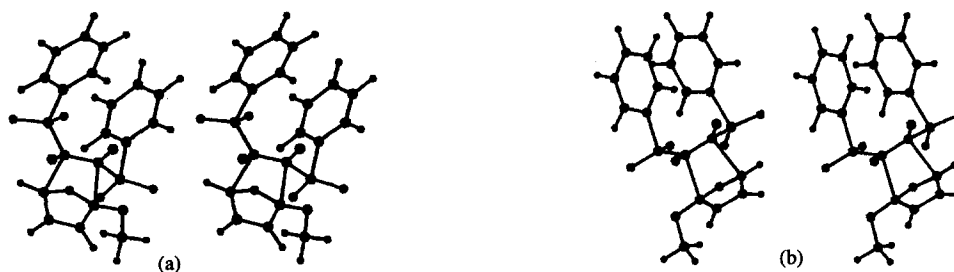


Fig. 7. Stereoview of energy minimum for the computed transition structures (in vacuum) for the 1/2b reaction after reparameterizing the MM3* force field: (a) structure producing 3b; (b) structure producing 4b.

Table 7. Main Geometrical Features Obtained for the TS between 2-Hydroxyfuran and Ethylene in *ab initio* and MM3* Calculations.

The image shows a 3D ball-and-stick model of the transition state between 2-hydroxyfuran and ethylene. The atoms are numbered from 1 to 16. Carbon atoms are grey, oxygen atoms are red, and hydrogen atoms are white. The structure shows the partial bonds between the furan ring and the ethylene fragment.

Bond Lengths								
Bond	<i>ab initio</i>	MM3*	Bond	<i>ab initio</i>	MM3*	Bond	<i>ab initio</i>	MM3*
1-2	1.381	1.363	3-6	2.200	2.200	6-13	1.088	1.088
1-3	1.416	1.412	3-10	1.353	1.349	6-15	1.085	1.086
1-8	1.081	1.101	4-5	1.383	1.376	7-12	1.087	1.088
2-4	1.416	1.434	4-7	2.138	2.138	7-14	1.086	1.087
2-9	1.082	1.102	4-11	1.082	1.088	10-16	0.971	0.946
3-5	1.372	1.362	6-7	1.396	1.389			

Bond Angles								
Angle	<i>ab initio</i>	MM3*	Angle	<i>ab initio</i>	MM3*	Angle	<i>ab initio</i>	MM3*
1-2-4	106.4	105.8	2-4-11	128.3	128.0	6-7-12	119.3	119.1
1-2-9	127.4	128.0	3-1-8	125.0	125.6	6-7-14	120.1	120.3
1-3-5	108.7	108.7	3-5-4	103.3	103.1	7-6-13	119.3	119.1
1-3-10	125.0	124.9	3-10-16	108.3	108.2	7-6-15	120.6	120.3
2-1-3	105.5	105.8	4-2-9	125.3	125.6	12-7-14	114.3	114.5
2-1-8	128.8	128.0	5-3-10	117.0	117.3	13-6-15	114.5	114.5
2-4-5	107.7	108.1	5-4-11	114.6	114.9			

Torsion Angles								
Angle	<i>ab initio</i>	MM3*	Angle	<i>ab initio</i>	MM3*	Angle	<i>ab initio</i>	MM3*
1-2-4-5	18.5	18.0	3-1-2-9	-170.6	-173.7	8-1-3-10	25.8	20.3
1-2-4-11	162.5	163.3	3-5-4-11	-177.8	-178.3	9-2-4-11	-27.7	-23.4
1-3-5-4	27.8	27.4	4-2-1-8	170.3	170.9	12-7-6-13	-0.5	-0.7
2-1-3-5	-16.9	-16.8	4-5-3-10	176.4	178.2	12-7-6-15	151.6	150.3
2-1-3-10	-162.3	-168.0	5-3-1-8	171.3	171.3	13-6-7-14	-151.0	-151.5
2-4-5-3	-28.3	-27.9	5-4-2-9	-171.7	-168.8	14-7-6-15	1.1	-0.6
3-1-2-4	-1.1	-0.7	8-1-2-9	0.8	-2.1			

Table 8. Computed Relative Energy (kcal mol⁻¹) and Population Analysis (in parenthesis, %) for the Different Transition Structures of Reaction between **1** and **2b**.

Reactant	Conformer	<u>In vacuum</u>		<u>GB/SA</u>	
		3b	4b	3b	4b
2b	1-c1	71.82 (0.0)	74.00 (0.0)	45.57 (0.0)	47.42 (0.0)
	1-c2	65.03 (0.5)	67.59 (0.0)	38.56 (3.5)	40.93 (0.1)
	1-c3	62.03 (85.6)	63.11 (13.8)	36.71 (80.7)	37.70 (15.2)
	1-c4	66.28 (0.1)	68.50 (0.0)	39.75 (0.5)	41.52 (0.0)

CONCLUSIONS

Results obtained from this work demonstrate the synthetic usefulness of substituted furans, especially those with substituents on position 2. Moreover, the MM3-transition state model has been proved to be efficient only if the electronic demand of the studied reaction is very similar to that of the model. Otherwise, more refined transition state model has to be computed to achieve reasonably acceptable results. Selectivity in the 2-substituted furans arose by interactions between the 2-substituent and the sulfonyl groups (steric repulsions with the *cis*-sulfonyl or long-range favourable interactions -electrostatic, dipolar, van der Waals- with the *trans*-sulfonyl). Molecular geometry and the spatial disposition of substituents in the 3-substituted furans clearly justify a decrease in the selectivity.

ACKNOWLEDGEMENTS

Financial support was obtained from DGES ('Ministerio de Educación y Cultura', Spain) through grants no. PB96-0641, and PB96-1181. The UAB is thanked for a fellowship to one of us (X.G.). The UCM is thanked for a predoctoral fellowship (F.I.). This research has been carried out using computers of CESCA and CEPBA, coordinated by C⁴ ('Centre de Computació i Comunicacions de Catalunya').

EXPERIMENTAL SECTION

General. Reagents and solvents were handled by using standard syringe techniques. IR spectra were recorded on a Perkin-Elmer 297 spectrophotometer. Dichloromethane was distilled over CaH₂ before use. ¹H NMR and ¹³C NMR were obtained on Varian XL-300, Bruker AM-250 and Bruker AM-300 spectrometers. Chemical shifts (δ) are reported in ppm from internal (CH₃)₄Si. Silica gel Merck 60 (230-240 mesh) and Merck 60F₂₅₄ plates were used for conventional and analytical (TLC) chromatography respectively. Melting points were determined on a Gallenkamp instrument and are uncorrected. Elemental analyses were performed at the Universidad Complutense de Madrid.

2-(benzyloxymethyl)furan (2d). To a solution of 2-(hydroxymethyl)furan (20 mmol) and TBAI (catalytic amount) in THF (200 ml), NaH (41 mmol) and benzylbromide (51 mmol) were added at 0 °C. The mixture was stirred 24 h. Then, H₂O was added and aqueous layer was extracted with diethylether. Organic phases were dried with MgSO₄, filtered and solvent was evaporated in vacuo. The crude was submitted to silica gel chromatography (Hex:AcOEt 20:1) and 3.63 g of furan **4b** were obtained (96 %) as a yellow oil: IR (KBr) 3010,

2920, 2850, 1470, 1360, 1150 cm^{-1} ; ^1H NMR (CDCl_3 , 300 MHz) δ 4.40 (s, 2 H, CH_2), 4.46 (s, 2 H, CH_2), 6.24–6.27 (m, 2 H, H-3, H-4), 7.20–7.34 (m, 6 H, H-5, CH_2Ph); ^{13}C NMR (CDCl_3 , 62.5 MHz) δ 63.9, 72.0, 109.5, 110.4, 127.8, 128.0, 128.5, 138.0, 143.0. Anal. Calcd. for $\text{C}_{12}\text{H}_{12}\text{O}_2$: C, 76.60; H, 6.38. Found: C, 76.43; H, 6.54.

3-(benzyloxymethyl)furan (5b). To a solution of 3-(hydroxymethyl)furan (1.02 mmol) and TBAI (catalytic amount) in THF (10.2 ml) at 0 °C, NaH (2.04 mmol) and benzybromide (2.55 mmol) were added. The reaction mixture was stirred for 24 h. and H_2O was added. The crude was extracted with diethylether and organic layer were dried under MgSO_4 , filtered and the solvent was eliminated under reduced pressure. The crude was submitted under silica gel chromatography (Hex:AcOEt 20:1) and 192 mg of furan **5b** were obtained as a yellow oil: IR (KBr) 3010, 2920, 2850, 1470, 1360, 1150 cm^{-1} ; ^1H NMR (CDCl_3 , 300 MHz) δ 4.24 (s, 2 H, CH_2), 4.36 (s, 2 H, CH_2), 6.29 (bs, 1 H, H-4), 7.10–7.26 (m, 7 H, H-2, H-5, CH_2Ph); ^{13}C NMR (CDCl_3 , 62.5 MHz) δ 63.5, 72.0, 110.6, 128.2, 128.2, 128.6, 140.9, 143.6. Anal. Calcd. for $\text{C}_{12}\text{H}_{12}\text{O}_2$: C, 76.60; H, 6.38. Found: C, 76.45; H, 6.50.

General procedure for Diels-Alder reactions. To a solution containing *E*-1,2-bis-(phenylsulfonyl)-ethylene **1** in CH_2Cl_2 (10 ml/mmol) were added three equivalents of furans **2** or **5**. The mixture was stirred at room temperature until the starting material was disappeared. The solvent was removed under reduced pressure and the residue was purified by silica gel chromatography, using the appropriate eluant in each case

6-endo-5-exo-bis-(phenylsulfonyl)-1-methyl-7-oxabicyclo[2.2.1]hept-2-ene (3a). Reaction (24 h) of **1** (0.16 mmol) with furan **2a** (0.48 mmol) in CH_2Cl_2 (4 ml) afforded, following the general procedure, and after silica gel chromatography (Hex:AcOEt 2:1) 62 mg (100%) of **3a**, as a white solid: mp 93–94 °C; IR (KBr) 3010, 1585, 1450, 1330, 1180, 1150, 1090, 790, 750 cm^{-1} ; ^1H NMR (CDCl_3 , 300 MHz) δ 1.77 (s, 3 H, Me), 3.79 (d, 1 H, $J=4.0$ Hz, H-5), 3.88 (d, 1 H, $J=4.4$ Hz, H-6), 5.21 (d, 1 H, $J=1.8$ Hz, H-4), 6.51 (dd, 1 H, $J=1.8, 5.5$ Hz, H-3), 6.64 (d, 1 H, $J=5.5$ Hz, H-2), 7.52–7.69 (m, 10 H, SO_2Ph); ^{13}C NMR (CDCl_3 , 75 MHz) δ 18.2, 70.2, 71.0, 80.4, 89.2, 128.3, 128.4, 128.8, 129.4, 129.9, 134.2, 134.2, 134.9, 140.3. Anal. Calcd. for $\text{C}_{19}\text{H}_{18}\text{O}_5\text{S}_2$: C, 58.46; H, 4.62. Found: C, 58.56; H, 4.75.

6-endo-5-exo-bis-(phenylsulfonyl)-1-methoxy-7-oxabicyclo[2.2.1]hept-2-ene (3b). Reaction (4 h) of **1** (1.6 mmol) with furan **2b** (4.9 mmol) in CH_2Cl_2 (16 ml) afforded 650 mg of **3b**, as a white solid (100 %): IR (KBr) 3000, 1750, 1500, 1450, 1300, 1210, 1150, 750, 680 cm^{-1} ; ^1H NMR (CDCl_3 , 300 MHz) δ 3.33 (s, 3 H, Me), 3.79 (d, 1 H, $J=4.8$ Hz, H-5), 4.00 (d, 1 H, $J=4.8$ Hz, H-6), 5.22 (d, 1 H, $J=1.8$ Hz, H-4), 6.60 (dd, 1 H, $J=1.1, 5.9$ Hz, H-3), 6.70 (d, 1 H, $J=5.9$ Hz, H-2), 7.45–7.50 (m, 4 H, SO_2Ph), 7.51–7.63 (m, 2 H, SO_2Ph), 7.69 (d, 2 H, $J=7.7$ Hz, SO_2Ph), 7.78 (d, 2 H, $J=8.1$ Hz, SO_2Ph); ^{13}C NMR (CDCl_3 , 62.5 MHz) δ 55.2, 65.2, 65.6, 68.9, 112.5, 126.9, 128.6, 128.8, 129.2, 129.3, 129.6, 130.0, 135.1, 140.4, 151.5. Anal. Calcd. for $\text{C}_{19}\text{H}_{18}\text{O}_6\text{S}_2$: C, 56.16; H, 4.43. Found: C, 56.30; H, 4.30.

6-endo-5-exo-bis-(phenylsulfonyl)-1-(hydroxymethyl)-7-oxabicyclo[2.2.1]hept-2-ene (3c) and 1-hydroxymethyl-5-endo-6-exo-bis-(phenylsulfonyl)-7-oxabicyclo[2.2.1]hept-2-ene (4c). Reaction (12 h) of **1** (0.06 mmol) and furan **2c** (0.19 mmol) in CH_2Cl_2 (1 ml) afforded, following the described procedure, and after column chromatography (Hex:AcOEt 5:1) an inseparable mixture of **3c** and **4c** (26 mg, 100%). Longer reaction time (19 h) afforded 24 mg of **3c** (100 %): mp 130–131 °C; IR (KBr) 3350, 2940, 1460, 1320, 1160, 1100, 770,

700 cm^{-1} ; $^1\text{H NMR}$ (CDCl_3 , 300 MHz) δ 3.83 (d, 1 H, $J=4.4$ Hz, H-5), 4.15 (d, 1 H, $J=12.9$ Hz, CH_2), 4.32 (d, 1 H, $J=13.6$ Hz, CH_2), 4.39 (d, 1 H, $J=4.0$ Hz, H-6), 5.36 (d, 1 H, $J=1.5$ Hz, H-4), 6.64 (dd, 1 H, $J=1.5, 5.5$ Hz, H-3), 6.68 (d, 1 H, $J=5.5$ Hz, H-2), 7.48–7.93 (m, 10 H, SO_2Ph); $^{13}\text{C NMR}$ (CDCl_3 , 75 MHz) δ 60.0, 64.0, 70.4, 80.8, 93.3, 128.2, 128.5, 128.9, 129.4, 134.4, 136.8. Anal. Calcd. for $\text{C}_{19}\text{H}_{18}\text{O}_6\text{S}_2$: C, 56.16; H, 4.43. Found: C, 56.26; H, 4.30.

1-(benzyloxymethyl)-6-endo-5-exo-bis-(phenylsulfonyl)-7-oxabicyclo[2.2.1]hept-2-ene (3d). Reaction (72 h) of 2.4 mmol of **1** with 7.2 mmol of furan **2d** in 24 ml of CH_2Cl_2 rendered 930 mg (78 %) of **3d**, after silica gel chromatography (Hex:AcOEt 10:1) as a white solid: mp 180–181 $^\circ\text{C}$; IR (KBr) 3080, 2960, 1750, 1460, 1325, 1160, 1110, 1090, 760, 700 cm^{-1} ; $^1\text{H NMR}$ (CDCl_3 , 300 MHz) δ 3.77 (d, 1 H, $J=4.4$ Hz, H-5), 3.87 (d, 1 H, $J=11.7$ Hz, CH_2), 4.24 (d, 1 H, $J=11.7$ Hz, CH_2), 4.36 (d, 1 H, $J=11.7$ Hz, CH_2), 4.37 (d, 1 H, $J=4.4$ Hz, H-6), 4.43 (d, 1 H, $J=11.7$ Hz, CH_2), 5.28 (s, 1 H, H-4), 6.55 (s, 2 H, H-2, H-3), 7.15–7.85 (m, 15 H, CH_2Ph , SO_2Ph); $^{13}\text{C NMR}$ (CDCl_3 , 62.5 MHz) δ 64.3, 67.0, 70.4, 73.4, 81.1, 92.6, 127.7, 128.2, 128.3, 128.4, 128.9, 129.2, 129.2, 129.8, 134.0, 134.1, 134.9, 136.7, 137.2, 140.3. Anal. Calcd. for $\text{C}_{26}\text{H}_{24}\text{O}_6\text{S}_2$: C, 62.90; H, 4.84. Found: C, 62.73; H, 4.68.

6-endo-5-exo-bis-(phenylsulfonyl)-1-(mercaptomethyl)-7-oxabicyclo[2.2.1]hept-2-ene (3e). Reaction (25 h) of **1** (1.6 mmol) with **2e** (4.9 mmol) in 16 ml of CH_2Cl_2 produced, after column chromatography (Hex:AcOEt 5:1) 684 mg (100 %) of **3e** as a white solid: mp 135–136 $^\circ\text{C}$; IR (KBr) 3330, 2920, 1580, 1480, 1450, 1320, 1180, 1150, 1080, 800 cm^{-1} ; $^1\text{H NMR}$ (CDCl_3 , 300 MHz) δ 1.16 (t, 1 H, $J=8.8$ Hz, SH), 3.24 (d, 2 H, $J=8.8$ Hz, CH_2), 3.74 (d, 1 H, $J=4.0$ Hz, H-5), 4.41 (d, 1 H, $J=4.4$ Hz, H-6), 5.26 (s, 1 H, H-4), 6.57 (s, 2 H, H-2, H-3), 7.38–7.83 (m, 10 H, SO_2Ph); $^{13}\text{C NMR}$ (CDCl_3 , 75 MHz) δ 26.1, 64.9, 71.3, 80.7, 92.8, 128.4, 128.6, 129.4, 129.5, 130.0, 134.4, 134.5, 135.1, 137.1, 138.4, 140.4. Anal. Calcd. for $\text{C}_{19}\text{H}_{18}\text{O}_5\text{S}_3$: C, 54.03; H, 4.26. Found: C, 53.90; H, 4.36.

6-endo-5-exo-bis-(phenylsulfonyl)-2-(hydroxymethyl)-7-oxabicyclo[2.2.1]hept-2-ene (6a) and 5-endo-6-exo-bis-(phenylsulfonyl)-2-(hydroxymethyl)-7-oxabicyclo[2.2.1]hept-2-ene (7a). Reaction (19 h) of 0.06 mmol of **1** with furan **5a** (0.19 mmol) in CH_2Cl_2 (1.3 ml) rendered a 6:4 mixture of **6a** and **7a** as white solids, after column chromatography (Hex:AcOEt 5:1) (20 mg, 76 %): $^1\text{H NMR}$ (CDCl_3 , 300 MHz) δ 3.56 (d, 1 H, $J=4.8$ Hz), 3.71 (d, 1 H, $J=4.4$ Hz), 4.09 (d, 2 H, $J=6.6$ Hz), 4.23 (t, 1 H, $J=4.4$ Hz), 4.26 (t, 1 H, $J=4.4$ Hz), 4.32 (d, 1 H, $J=14.3$ Hz), 4.42 (d, 1 H, $J=14.3$ Hz), 4.58–4.60 (m, 2 H), 5.24 (d, 1 H, $J=4.4$ Hz), 5.30 (s, 1 H), 5.33 (d, 1 H, $J=4.4$ Hz), 5.39 (d, 1 H, $J=1.1$ Hz), 6.43 (d, 1 H, $J=1.8$ Hz), 6.54 (dd, 1 H, $J=1.5, 2.9$ Hz), 7.38–7.93 (m, 30 H); $^{13}\text{C NMR}$ (CDCl_3 , 75 MHz) δ 58.0, 59.5, 67.1, 67.8, 67.9, 77.2, 80.5, 82.7, 82.8, 83.7, 128.2, 128.4, 128.5, 128.6, 129.5, 129.5, 129.9, 130.9, 131.0, 134.4, 134.4, 134.4, 134.6, 134.9, 137.6, 137.9, 138.7, 140.3, 149.6, 152.7.

2-(benzyloxymethyl)-6-endo-5-exo-bis-(phenylsulfonyl)-7-oxabicyclo[2.2.1]hept-2-ene (6b) and 2-(benzyloxymethyl)-5-endo-6-exo-bis-(phenylsulfonyl)-7-oxabicyclo[2.2.1]hept-2-ene (7b). Reaction (47 h) of **1** (0.08 mmol) with furan **5b** (0.24 mmol) in CH_2Cl_2 (0.8 ml) produced a mixture of **6b** and **7b** (35 mg, 87 %) as white solids, after silica gel chromatography (Hex:AcOEt 5:1): $^1\text{H NMR}$ (CDCl_3 , 300 MHz) δ 3.64 (d, 1 H, $J=4.8$ Hz), 3.70 (d, 1 H, $J=4.8$ Hz), 4.19–4.22 (m, 3 H), 4.29 (t, 1 H, $J=4.4$ Hz), 4.41–4.52 (m, 4 H), 4.55 (d, 1 H, $J=12.1$ Hz), 4.64 (d, 1 H, $J=11.8$ Hz), 5.24 (d, 1 H, $J=4.4$ Hz), 5.31 (d, 1 H, $J=4.4$ Hz), 5.32 (d, 1 H, $J=1.5$ Hz), 5.36 (d, 1 H, $J=1.5$ Hz), 6.46 (d, 1 H, $J=1.5$ Hz), 6.52 (d, 1 H, $J=1.5$ Hz), 7.29–7.74 (m, 30 H); $^{13}\text{C NMR}$

NMR (CDCl₃, 75 MHz) δ 64.6, 64.8, 66.6, 66.9, 67.5, 68.0, 72.6, 72.6, 80.0, 80.4, 82.4, 82.9, 127.6, 127.7, 127.7, 127.8, 128.2, 128.4, 128.4, 128.5, 128.6, 129.4, 129.4, 131.0, 131.4, 134.2, 134.3, 134.3, 136.8, 137.6, 137.8, 137.9, 139.0, 139.1, 147.4, 149.6.

REFERENCES

1. For a recent review, see Kappe, O. C.; Murphree, S.; Padwa, A. *Tetrahedron* **1997**, *53*, 14179. For some recent references, see: a) Kumar, S. A.; Balasubrahmanyam, S. N. *Tetrahedron Lett.* **1997**, *38*, 1099. b) Adrio, J.; Carretero, J. C.; García-Ruano, J. L.; Martín-Cabrejas, L. M. *Tetrahedron: Asymmetry*, **1997**, *8*, 1623. c) Butz, T.; Saver, J. *Tetrahedron: Asymmetry* **1997**, *8*, 703. d) Evans, D. A.; Barnes, D. M. *Tetrahedron Lett.* **1997**, *38*, 57. e) Lautens, M.; Fillion, E. *J. Org. Chem.* **1997**, *62*, 4418. f) Jeanneret, V.; Meerpoel, L.; Vogel, P. *Tetrahedron Lett.* **1997**, *38*, 543. g) Mossimann, H.; Vogel, P.; Pinkerton, A.; Kirschbaun, K. *J. Org. Chem.* **1997**, *62*, 3002. h) Toyota, A.; Uchiyama, M.; Kanako, C. H. *Tetrahedron* **1997**, *53*, 6327. i) Vitti, G.; Perrotta, E.; Giannotti, D.; Namicini, R. *Tetrahedron*, **1997**, *53*, 8519. j) Lai, Y. H.; Yong, Y. L. Wong, S. W. *J. Org. Chem.* **1997**, *62*, 4500. k) Elliot, R. L.; Nicholson, N. H.; Peaker, F. E.; Takle, A. K.; Richardson, C. M.; Tyler, J. W.; White, J.; Pearson, M. J.; Eggleston, D. S.; Haltiwanger, R. C. *J. Org. Chem.* **1997**, *62*, 4998. e) Lautens, M.; Ma, S.; Chiu, P. *J. Am. Chem. Soc.* **1997**, *119*, 6478.
2. De Lucchi, O.; Lucchini, V.; Pasquato, L.; Modena, G. *J. Org. Chem.* **1984**, *49*, 596.
3. Aceña, J. L.; Arjona, O.; Iradier, F.; Plumet, J. *Tetrahedron Lett.* **1996**, *37*, 105.
4. Aceña, J. L.; Arjona, O.; Plumet, J. *Tetrahedron: Asymmetry* **1996**, *7*, 3535.
5. MacroModel version of Allinger's MM3: Allinger, N.L.; Yuh, Y.H.; Lii, J-H. *J. Am. Chem. Soc.* **1989**, *111*, 8551.
6. Polak, E.; Ribiere, G. *Rev. Fr. Inf. Rech. Oper.* **1969**, *16*, 35.
7. a) Brown, F.K.; Houk, K.N. *Tetrahedron Lett.* **1984**, *25*, 4609. b) Brown, F.K.; Houk, K.N. *Tetrahedron Lett.* **1985**, *26*, 2297. c) Eksterowicz, J. E.; Houk, K.N. *Chemical Reviews* **1993**, *93*, 2439.
8. MacroModel V5.0; Mohamda, F.; Richards, N.G.J.; Guida, W.C.; Liskamp, R.; Caufield, C.; Chang, G.; Hendrickson, T.; Still, W.C. *J. Comput. Chem.* **1990**, *11*, 440.
9. Dr. V. Branchadell is thanked for providing the coordinates of the transition state structure.
10. Brown, F. K.; Houk, K. N.; Burnell, D. J.; Valenta, Z. *J. Org. Chem.* **1987**, *52*, 3050.
11. Still, W.C.; Tempczyk, A.; Hawley, R.C.; Hendrickson, T. *J. Am. Chem. Soc.* **1990**, *112*, 6127.
12. Hunter, C.A.; Sanders, J.K.M. *J. Am. Chem. Soc.* **1990**, *112*, 5525.
13. Jorgensen, W.L.; Severance, D.L. *J. Am. Chem. Soc.* **1990**, *112*, 4768.
14. Becke3lyp from DFT methods with a 6-31G* basis set.
15. *Stretching parameters*: T1-T2 (2.138 Å, 999.99 mdyne/Å, 0. debye); T1-T2(O3H2) (2.200 Å, 999.99 mdyne/Å, 0. debye). *Bending parameters*: C2-T2-O3(H2) (125.0°, 10. mdyne/rad², 0.24 mdyne/rad²); T1-T2-O3(H2) (110.1°, 10 mdyne/rad², 0.24 mdyne/rad²); O3-T2-O3(H2) (117.2°, 10 mdyne/rad², 0.24 mdyne/rad²); T2-O3-H2 (108.3°, 10 mdyne/rad², 0.3 mdyne/rad²).